PHYSICAL REVIEW B **68**, 125206 (2003)

Limitations of electrical detection of x-ray absorption fine structure

J. Bollmann,* S. Knack, and J. Weber
Technische Universität Dresden, D-01062 Dresden, Germany

V. Koteski and H.-E. Mahnke
Hahn-Meitner-Institut Berlin GmbH, D-14109 Berlin, Germany

E. Welter
Hamburger Elektronen Synchrotron (HASYLAB) at Deutsches Elektronen Synchrotron (DESY), D-22607 Hamburg, Germany

(Received 10 April 2003; revised manuscript received 5 August 2003; published 26 September 2003)

A scheme of capacitance detection for the x-ray absorption fine structure (XAFS) has recently been reported [M. Ishii, Phys. Rev. B **65**, 085310 (2002)]. The scheme was intended to expand the applicability of XAFS to study defect centers with deep electronic states within the band gap of a semiconductor. In addition to the proposed measurement of the steady-state capacitance, we introduce the new detection of capacitance transients. The possibilities and limits of the different electrical detection methods are discussed. Special attention is given to the question whether XAFS detected by capacitance can selectively analyze strongly diluted defects. The XAFS at the *K* edge of gallium and arsenic is measured on GaAs and AlGaAs Schottky diodes containing donor related deep level defects (DX center) and $\mathrm{Al}_{\mathrm{Ga}}$ antisite detects (EL2 center). The oscillation in x-ray absorption is electrically detected by monitoring (i) the photocurrent under short circuit conditions, (ii) the steady-state impedance, and (iii) x-ray-induced capacitance transients. We do not find any significant differences between the electrically and conventionally detected XAFS spectra. From our experimental data and estimates we find no evidence for a site selectivity of capacitance XAFS.

DOI: 10.1103/PhysRevB.68.125206 PACS number(s): 61.72.Ji, 78.70.Dm, 61.10.Ht, 71.55.Eq

I. INTRODUCTION

X-ray absorption fine structure (XAFS) (Refs. 1 and 2) near the absorption edges of inner atomic shells reveals detailed information on the microscopic environment of an element in the solid state.[3,4] Today, theory[5,6] is able to model the scattering process of the emitted electron so that from precise experimental data, information can be obtained about the coordination, the number and distances of atoms in the nearest-neighbor shell, the next nearest neighbor, and even higher-order neighbor shells. The technique is well established and often applied to identify chemical elements in the bulk and at surfaces, and reveal the structure and the composition of solids as well as structural phase changes.

The properties of point defects in semiconductors are of great importance in device processing, because they often determine material properties even in concentrations as low as $10^{15}\ \mathrm{cm}^{-3}$. The method of XAFS analysis is ideally suited to determine coordination and local structure of defects.[3] Unfortunately, the x-ray absorption on highly diluted defects is obscured by the high-absorption background from elastic scattering and from photoionization at other elements and/or higher atomic shells. So far, the improvements in synchrotron sources as well as in detection techniques allows one to go down to around $10^{18}\ \mathrm{cm}^{-3}$ in defect concentration and even lower under optimal conditions. For example, local structure studies have been reported for various dopants in Si at a level of a few times $10^{18}\ \mathrm{cm}^{-3}$.[7,8] A further increase in sensitivity to reach lower concentrations is highly desirable.

Alternative techniques sensitive to defect-specific properties (e.g., the charge state of a deep-level defect) are routinely used in studies of semiconductors.[9] Most prominent are capacitance transient methods such as deep-level transient spectroscopy.[10] Such electrical methods applied to bipolar devices or Schottky junctions make use of thermally stimulated changes of charge states of deep-level centers. As a thermal spectroscopy, their spectral resolution is limited but their sensitivity is extremely high.[10] Defect concentrations as low as $10^{10}\ \mathrm{cm}^{-3}$ can be detected. However, no information beyond the electrical activity and the carrier capture cross section is revealed.

On the other hand, the fine structure of the x-ray absorption at an inner shell of an atom depends on the electronic and geometric configuration of this atom in a solid. Atoms will give XAFS signals that are specific to their lattice sites.[11,12] If different atoms occupy different (inequivalent) positions in a solid, the XAFS result will be a superposition of the absorption from all the different sites. Recently, a *site-selective* scheme of capacitance detection for XAFS has been proposed by Ishii and co-workers.[13–15] The site selectivity allows the selection of just one of the different lattice positions by monitoring a signal which is related to the x-ray absorption of just this site and suppressing all other contributions from other sites. In the case of intrinsic defects such as antisite defects, this allows the selective measurement of the x-ray absorption at defect atoms, and provides information which is normally hidden under the dominant absorption of the undisturbed host atoms.

Our study was initiated by the intriguing possibilities of the reported site-selective XAFS detection by capacitance measurements. We present here XAFS experiments on Se-doped $\mathrm{Al}_x\mathrm{Ga}_{1-x}\mathrm{As}$ containing DX centers[17,16] and GaAs containing EL2 centers.[18–20] Standard fluorescence and

0163-1829/2003/68(12)/125206(9)/$20.00

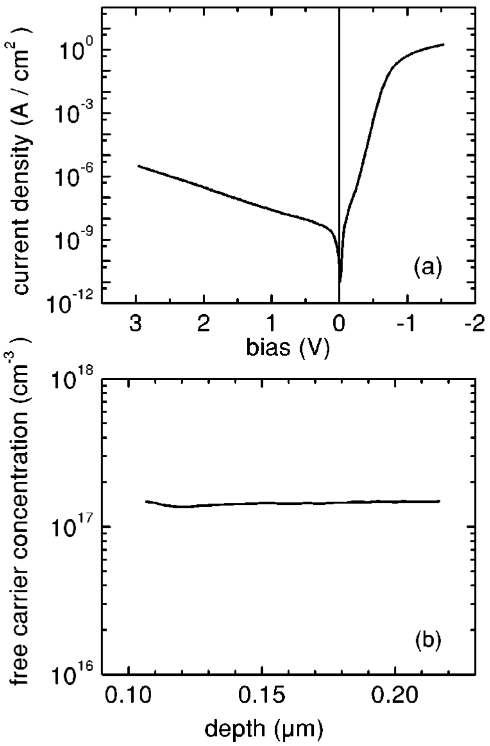

FIG. 1. Electrical properties of the $Al_xGa_{1-x}As$ ($x=0.3$) Schottky barrier diode, (a) current-voltage characteristic in the dark, and (b) shallow doping density from *CV* profiling.

transmission methods as well as different schemes for electrical detection of the XAFS spectra are applied and the results compared. A detailed discussion of the electrically detected XAFS spectra is presented. The physical processes which give rise to the different signals are discussed in detail.

II. EXPERIMENT

A. Sample characteristics

Our experiments were performed on two sets of samples. One set had thin layers (5 μm) of $Al_xGa_{1-x}As$ ($x=0.3$) grown by molecular-beam epitaxy on highly conductive GaAs substrates doped with Se. The other set was (100)-oriented, virtually gradient-free grown, *n*-type bulk GaAs from MCP Wafer Technology Ltd., nominally undoped.

The free-electron concentration is 1.3×10^{17} cm^{-3} in the epitaxial layers and 2.5×10^{16} cm^{-3} for the bulk GaAs samples. Backside Ohmic contacts were fabricated by GaAs standard technology and Schottky barrier diodes prepared by high vacuum deposition of Ti/Au layers. The contact diameters of the diodes varied from 0.2 to 1 mm. The electrical characterization of a typical Schottky barrier diode is given in Fig. 1. The diodes meet the condition for impedance measurements with a reverse leakage current smaller than 10^{-8} A and a series resistance (determined from forward current) of 1.2 $k\Omega$. The DX center in the $Al_xGa_{1-x}As$ layers was found to be the dominating defect, which was distributed homogeneously with a density of 10^{16} cm^{-3}. The EL2 concentration in the bulk GaAs was 4×10^{15} cm^{-3}.

B. Experimental methods

X-ray absorption spectra were measured at DESY (HASYLAB), Hamburg. The experiment was set up in the A1 beamline which uses a channel-cut Si(111) crystal as monochromator which covers an energy range from 3 to 17 keV.[21] A cryostat was installed for the in-beam photocurrent and impedance measurements at low temperatures. All experimental data presented here were measured at 80 K. Conventional XAFS was measured in transmission mode with ionization chambers, in fluorescence mode with a five-element Ge detector, and with total e^--yield detection using a Keithley current meter model 617. The diodes were held under zero-bias and short circuit condition to minimize the influence of dark currents for photocurrent detection. The noise level for the direct current measurement was about 0.5 pA, well below the x-ray-induced photocurrents, which are of the order of several 100 pA. For impedance measurements, the diodes were reverse biased and either the steady-state impedance or the capacitance transient of the diode under irradiation as a function of x-ray energy was measured. For the capacitance measurements we used the *LCR* meter HP4194A from Hewlett-Packard. All impedance measurements were carried out under high-frequency conditions to avoid the admittance from deep levels, due to the in-phase capture and emission of carriers. The high-frequency amplitude was chosen to be comparable to the thermovoltage (kT/q) keeping the distortion of the steady-state impedance by the high-frequency voltage smaller than the spreading of the space-charge edge (Debye tailing effect). The impedance is usually interpreted either as a resistor R_s in series to a capacitor C_s or a resistor R_p parallel to a capacitor C_p.[9] These simple networks are an appropriate description of the Schottky barrier diode and can be easily checked by comparing the results obtained for different measurement frequencies.

Capacitance transients induced by the x-ray irradiation were recorded under fixed reverse bias in darkness. The deep-level centers within the space-charge region were filled with majority charge carriers by reducing the reverse bias for a short time (filling pulse). This procedure is identical to photocapacitance measurements or minority-carrier transient spectroscopy.[22] Instead of illumination with photons with sub-band-gap or inter-band-gap transition energies, x-rays are used here. In our experiments, the trap filling was done under continuous irradiation because the x-ray-induced emission rate is negligible. The capture rate during filling is several orders of magnitude larger and ensures the complete occupation of the deep-level centers. The x-ray-induced emission after filling is measured at sample temperatures where the thermal emission from the traps can be neglected. For the EL2 defect this condition is fulfilled for temperatures below 150 K.

III. RESULTS

A. X-ray absorption of GaAs

EL2 is the dominant defect in unintentionally or low doped *n*-type GaAs. It behaves as a deep electron trap with a

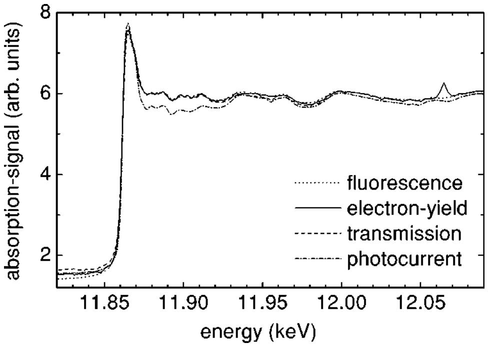

FIG. 2. X-ray absorption spectra at the *K* edge of As in bulk GaAs detected by different techniques.

thermal activation energy of $E_C - E_T = 0.86$ eV. This defect has been characterized extensively by capacitance spectroscopy.[20,19] The cross sections for both hole and electron capture at the defect are well established and make this defect an ideal subject to test the capacitance-XAFS technique.

The ''regular'' absorption spectra at the *K* edge of As and Ga were detected in transmission, by fluorescence, and total electron yield. Figure 2 shows the results for the absorption around the As *K* edge. As expected, all spectra show the same structure with minor differences due to different background behavior. In the figure, the energy scale is adjusted to the standard As *K*-absorption edge.

Capacitance transients of the GaAs Schottky barrier diodes under x-ray irradiation were recorded according to the procedure described in Sec. II B and the corresponding time constants were determined. The sample was held at 80 K for these measurements and the x-ray energy was varied from 11.852 keV to 11.880 keV in steps of 2 eV. Three individual transients are shown in Fig. 3. The x-ray irradiation leads to a change in the charge state of the EL2 level. The variation of the absorption at the *K* edge of As results in a corresponding variation of the emission rates indicated by a shift of the different capacitance transients on the time axis. Reference measurements in the dark without x-ray irradiation showed no capacitance transients. This proves that thermal emission from the deep level can be neglected and the x-ray irradiation indeed causes the observed capacitance transients.

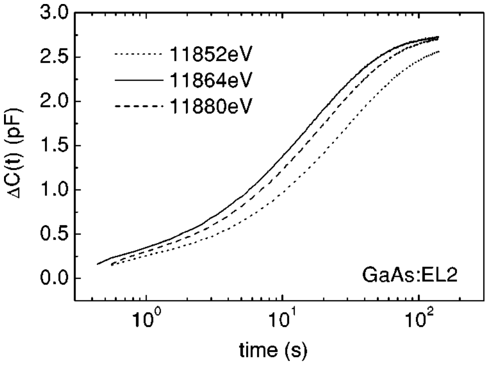

FIG. 3. Capacitance transients induced by x-ray energies lower, equal, and above the *K* edge of As in GaAs.

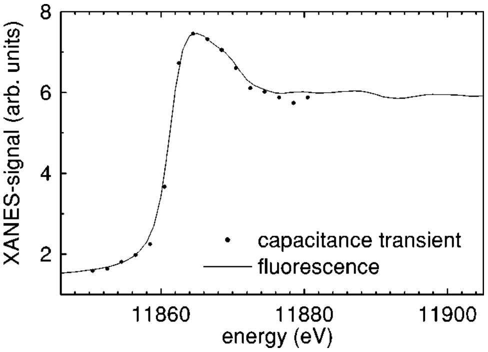

FIG. 4. Comparison of x-ray-induced capacitance time constants with the fluorescence spectrum near the *K* edge of As in bulk GaAs.

If the emission time constants of the transients are plotted against the x-ray energy, a XAFS spectrum is again obtained. The results in the near-edge region are shown in Fig. 4.

For comparison, the fluorescence spectrum is given for the same spectral region. Obviously, the same absorption fine structure is measured independently of the detection technique.

B. X-ray absorption of $Al_xGa_{1-x}As$

The capacitance-XAFS technique has been recently demonstrated by Ishii on Schottky barrier diodes on $Al_{0.33}Ga_{0.67}As$ containing the DX center.[15] To reexamine his results, we selected an identical material in our experiments. Figure 5 shows the XAFS spectra of the absorption as detected by capacitance under fixed bias and of the short-circuit photocurrent of the Schottky barrier diode. As in the case of GaAs (Fig. 2), no significant differences in the full spectra are observed. The XAFS function $\chi(k)$, where k is the wave vector of the emitted photoelectron, is obtained from the measured absorption spectra by subtracting the smoothly varying atomiclike absorption and normalizing the net increase at the edge following standart XAFS spectra evaluation procedures by using the code AUTOBK.[23]

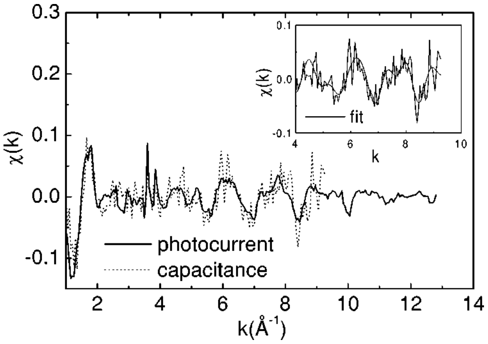

FIG. 5. XAFS function $\chi(k)$, measured as steady-state capacitance and as photocurrent of a Schottky barrier diode on *n*-type $Al_xGa_{1-x}As$:Se ($x = 0.3$). The original energy spectra were taken near the Ga absorption *K* edge ($V = 0$ V, $f = 5$ MHz). The inset shows an enhanced fraction of the capacitance signal. The solid line was obtained with the same parameters as those used to fit the photocurrent data (Sec. IV A).

The photocurrent is a measure of the total absorption, which is primarily due to the atoms of the host matrix. From Fig. 5, it is obvious that in terms of signal to noise, photocurrent measurements are highly superior. The crucial question is whether the capacitance signals widely suppress the capacitance signals from regular host atoms, thus enhancing selectively the signals originating from selected sites, e.g., special defect configurations. From our analysis, we demonstrate that capacitance and photocurrent signals are identical within the experimental error. The capacitance spectrum shows the expected energy of the Ga (K) edge as well as a fine structure due to Ga atoms on undisturbed lattice sites in an almost perfect $Al_xGa_{1-x}As$ crystal (see Sec. IV A). Our results give no support to the work of Ishii[15] who reported clear differences between the capacitively detected XAFS and the standard detection techniques.

IV. DISCUSSION

A. Conventional analysis of XAFS spectra

Our results show that the same fine structure is observed, independent of the detection technique. For a better characterization of our samples on a local scale and for a more quantitative comparison, we have fully analyzed the fluorescence spectrum for GaAs and the photocurrent spectrum for AlGaAs as well as the capacitance spectrum following the standard XAFS spectra evaluation procedures using the FEFF8 and FEFFIT code from the University of Washington software package.[24] In the program, theoretical standards are calculated for the backscattering amplitudes and phase shifts corresponding to the given atomic arrangements. Structural parameters such as interatomic distances, as well as mean-square displacements, and, if not known, coordination numbers can thereby be extracted from fits to the experimental data. Typically, the fit is performed in real space, which is obtained from Fourier transforming the $\chi(k)$ function.

In the case of the mixed system AlGaAs, we have measured the absorption at the Ga and the As K edge. Taking advantage of the capability of the FEFFIT program to fit multiple datasets, we were able to fit the combined data, thus reducing the number of free parameters and substantially decreasing correlations between various variables. The analysis was done by superposing contributions from the pure systems AlAs and GaAs according to their nominal weights x and $(1-x)$, respectively. This leaves as free parameters (for both absorption edges) all the relevant distances and corresponding mean square displacements, in addition to the inherent XAFS parameters (the starting energy of the photoelectron E_0 and the ''many-body'' electron reduction factor $S_0{}^2$).

With Ga as the central atom, the first coordination shell consists of tetrahedrally bound As atoms, while the second shell is a superposition of a Ga and an Al shell. The third shell has been treated as a single As shell since the distances in AlGaAs are known to be identical within our accuracy.[25] This procedure has been successfully applied to the mixed system CdZnTe.[26] The resolution of our data always allows us to include the first, second, and third coordination shells into our fit. In the case of distances between any combination of Ga and As atoms, the fit results agreed with the known distances within our error bars ($<1\%$). For combinations involving the less abundant Al, the errors were around 2%, again in agreement with the known values. Results of XAFS function $\chi(k)$ compared with least squared fits are shown in Figs. 6(a) and 6(b), respectively, for bulk AlGaAs and GaAs. The least-squares fit reproduces precisely the well-established structure of the perfect AlGaAs and GaAs lattice.

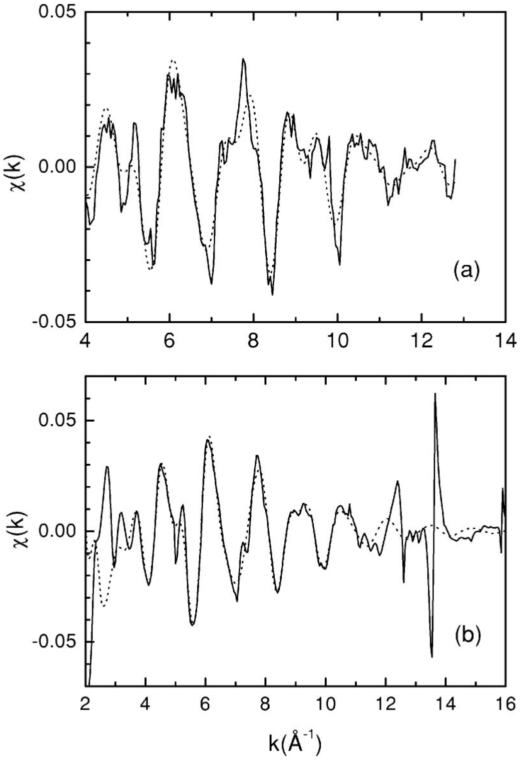

FIG. 6. XAFS function $\chi(k)$ for the Ga edge in $Al_xGa_{1-x}As$:Se ($x=0.3$) at 80 K (a); and for the As K edge in GaAs (dotted: fit; solid: experiment) (b).

In the case of the capacitance-detected absorption spectra shown in Fig. 5, the fit included in the insert was obtained by taking the parameters from the fit to the photocurrent spectrum. This leaves as free parameters only the first- and second-shell distances and the overall ''amplitude'' factor $S_0{}^2$. All three turn out to be in full agreement with the values from the photocurrent spectrum. Thus, we have to conclude that the capacitance-detected absorption does not result from an enhanced signal of a selected configuration (''site selectivity'') but rather reflects the local configurations of the Ga atoms in the bulk.

In the following, we want to discuss in detail the different modes of electrical detection with emphasis on a possible site selectivity.

B. Electrical detection of x-ray absorption fine structure

1. Elementary processes associated with x-ray absorption

X-ray absorption fine structure was first detected in transmission experiments.[27,28] The elementary processes in the interaction of x rays with material are (i) scattering (Compton and Rayleigh scattering), (ii) pair production, and (iii) atomic absorption causing electron emission (photoeffect) and a relaxation of the excited atom by Auger and secondary-electron or fluorescence photon emission. The probability for fluorescence or Auger relaxation depends on the charge of the nucleus and is roughly equal for *K*-shell absorption on Ga and As atoms.

The absorption process (iii) leads to the generation of a hole in an inner shell of the absorbing atom. The energy of the hole matches the binding energy of the electron (in our experiments about 10 keV). The energy that is absorbed in this process is dissipated via different channels. The core hole will relax radiatively giving rise to fluorescence or nonradiatively by an Auger process.

Near the surface, the Auger electrons and the primary electrons are able to escape from the sample. Both the fluorescence and these electrons can be used for the detection of XAFS spectra. Inside the samples the energy of the hole is dissipated mainly by impact ionization and in the end electron-hole pairs at the energy gap of the semiconductor are formed. Roughly, for one relaxing core hole of about 10 keV, several thousand electron-hole pairs will be generated.

2. X-ray-induced photocurrent

The detection of the x-ray absorption fine structure by induced currents in diodes is an old but seldom realized technique because it requires suitable space-charge structures which can only be fabricated for semiconductor materials. Early reports on measurements of XAFS spectra on GaAs diodes show that the fluorescence signal and the photocurrent contain the same information if appropriate corrections are applied.[29] Furthermore, XAFS detection by x-ray stimulated photoconduction of bulk crystals was reported.[30] Once again the technique yields the same information if corrections with respect to samples thickness are taken into account.

As mentioned above, the core holes inside the sample will create electron-hole pairs. In a neutral solid these pairs will recombine quickly. In contrast, within the space-charge region of a diode the electric field separates and sweeps out electrons and holes before a significant recombination can occur. The photocurrent generated directly in the space-charge region is, however, negligible, because the penetration of x rays is much deeper than the space-charge width of the junction (about 1 μm). The dominant part of the photocurrent originates from minority charge carriers generated in the bulk, which diffuse over a diffusion length of some 10 μm to the edge of the depletion region and are drifted throughout that layer to the metal electrode.

The photocurrent is, under continuous irradiation, a direct current. The alternating current, arising from an applied high-frequency voltage to measure the admittance of the Schottky barrier diode, is in general independent from this direct photocurrent. It is incorrect to associate the photocurrent with the real part of a complex alternating current.[15] The photocurrent, which is always present whether the direct-current or alternating-current properties of the diode under illumination are measured, is a direct current without a phase relation to the external alternating voltage and is therefore neither the real nor the imaginary part of the complex current. Yet, the photocurrent influences the admittance by introducing a current source into the complex two-pole network of the diode as discussed in the following section.

3. Changes in the steady-state capacitance due to x-ray irradiation

As shown in Sec. III B, the x-ray irradiation not only induces a photocurrent, but also leads to changes in the diode capacitance. By phase-sensitive measurements of the alternating currents at a small applied alternating bias, one estimates the parameters of the overall sample as an electrical network with an imaginary and a real part. Such data are easily interpreted, if the sample is a passive two-pole network dominated by its imaginary part. The system only behaves passive if no energy from radiation, magnetic fields, temperature gradients, pressure, or stress fields is added. In that case the reactance can be identified and interpreted as the differential space-charge capacitance of the diode, provided that small series resistors R_s arising from bulk conductivity and back contacts, as well as large parallel resistors R_p (e.g., small leakage currents) are given. The conductance is small and cannot be used to describe the influence of photocurrents on the parameters of the network. Under these conditions the influence of leaking currents (in the dark) to the differential capacitance can be simply estimated. If it is so small that the network is still dominated by the reactance $(R_p \gg 1/\omega C)$, the potential drop over R_s increases, thus the internal potential drop over the space-charge region decreases and the capacitance increases.[31] Since our Schottky barrier diodes have series resistors of about 1 $k\Omega$, this effect can be neglected for currents lower than 1 nA because minute potential shifts of $\sim\mu$V are expected. The corresponding variations in the capacitance are much less than 1 nF.

Under irradiation, the Schottky barrier diode becomes an active two-pole network with a more complex behavior. For some special cases some limits of expectations can be given.

Let us first assume an ideal Schottky barrier diode. The photocurrent j_{photo} has to be added to the network as a current source in parallel with the capacitance, and now the total current density j_{total} is given by

$$j_{total} = j_{diode} - j_{photo}.$$

Taking into account the dependence of j_{diode} on the (internal) voltage U over the depletion layer,

$$j_{diode} = j_0[\exp(U/U_T) - 1],$$

one obtains for the open circuit photovoltage U_{open}, i.e., $j_{total} \equiv 0$,

$$U_{open} = U_T \ln(j_{photo}/j_0 + 1). \tag{1}$$

Note that j_0 contains all material and junction specific parameters as, e.g., Schottky barrier height or band-gap energy for *pn* junctions. From current-voltage measurements (see Fig. 1), this saturation current can be estimated experimentally. From Eq. (1), the actual voltage over the depletion layer is obtained as a function of the photocurrent. Thus, independent of the operation mode of the diode (open or short circuit conditions), the capacitance increases with increasing photocurrent because of the decreasing depletion width. The capacitance of a Schottky barrier diode of a homogeneously doped semiconductor is given by

$$C_0^2 = qN_d \epsilon\epsilon_0/2U_0,$$

where U_0 is the internal bias over the depletion layer. For small changes in capacitance caused by bias variation ΔU, that is, with

$$\frac{C(U+\Delta U)^2}{C_0^2} - 1 \cong \frac{2[C(U+\Delta U)-C_0]}{C_0} = 2\frac{\Delta C}{C_0},$$

one obtains for the depletion layer

$$\Delta C/C_0 = 0.5\left(1 - \frac{1}{1+\Delta U/U_0}\right). \tag{2}$$

For real diodes, serial as well as parallel resistors influence the potential variations at the depletion layer and always result in suppressed variations of the potential.

Under the conditions discussed above, the reverse biased diode is dominated by the differential capacitance $C = dQ/dU$ of the depletion layer. Any additional contributions to the capacitance from deep-level centers, in the depletion region and the bulk or from the modulation of stored minority charges in bulk (diffusion capacitance), can be neglected. Indeed, the density of the deep-level centers is at least one order of magnitude lower than the doping concentration. Further, unipolar junctions do not have a significant diffusion capacitance.

We also measured the capacitance of our AlGaAs sample in the dark and under illumination. Instead of x rays, a white light source was used. The intensity of the light was tuned so that the stimulated photocurrents are comparable to those in the XAFS experiments. In our Schottky diodes, j_0 was 10^{-9} A cm^{-2} and j_{photo} under x-ray illumination was about 10^{-8} A cm^{-2}. From that, a potential change of 20 mV is expected and results in a capacitance change of up to 1%, as observed in the experiment. In excellent agreement in both experiments, the capacitance shift was determined to be 0.25 pF at about 150 pA photocurrent.

From the above discussion, we conclude that it is the photocurrent which is responsible for the changes in the steady-state capacitance. Therefore, the capacitance-XAFS spectrum does not contain additional information than what is obtained from the measured x-ray-induced photocurrent. Both techniques give XAFS spectra related to the bulk absorption of x rays. This conclusion is in agreement with our experimental finding that, within the experimental errors, both techniques give identical XAFS spectra.

Ishii and co-workers[13–15] give another explanation for the change of the steady-state capacitance. They claim that the photoionization of the defect centers is responsible. As they note, the defects are already ionized inside the space-charge region and cannot emit electrons anymore. However, in the bulk, any ionized trap will be immediately refilled. In their argument, only filled traps in the λ layer are responsible for the capacitance change. Yet, if the charge concentration in the λ layer increases, the edge of the space-charge region shifts towards the Schottky contact. In response, the applied voltage drops over a shortened distance. In effect, the ionized trap then lies within the neutral bulk and are refilled again. The dynamic equilibrium between ionization and refilling shifts the width of the space-charge region only for a small fraction of the Debye length. This process is therefore not effective in creating a capacitance change. This will become even more evident in the following section, where the time constants of the different processes are discussed.

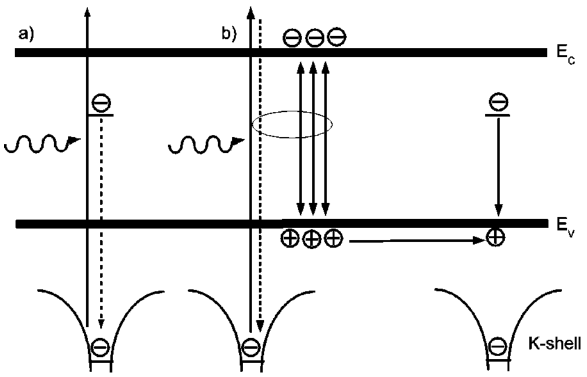

FIG. 7. (a) Change of the occupation of a defect level by a site-selective, direct absorption at the defect and successive capture of the defect electron. (b) Inner-shell absorption of x rays and subsequent generation of diffusing electron-hole pairs. Recombination of minority carriers with the defect electrons in the space-charge region.

4. X-ray-induced capacitance transients

The detection of the time constant from capacitance transients as a function of x-ray energy establishes a different way of measuring XAFS. The capacitance transient monitors changes of the trap occupation of deep-level centers inside the depletion region of a Schottky barrier diode. Under fixed bias, this change in space-charge density causes a corresponding capacitance transient. The observable time constant depends on the defect parameters and the ionization mechanism of the deep-level center. From the occurrence, amplitude, or direction of a capacitance transient itself, one cannot deduce the underlying physical process. Only a calculation of the expected time constants specific to the experimental conditions and defect parameters can clarify which physical process dominates.

The direct ionization of the defect level is the dominant absorption process in photocapacitance spectroscopy with photons that have energies below or near band gap. For the discussed x-ray energies, this direct absorption process lacks the specific structure of the inner-shell absorption. No absorption fine structure is therefore associated with this transition and we will exclude this process from the following discussion.

The two absorption processes (a) and (b) shown in Fig. 7 can lead to the observed capacitance transients. In (a), the x rays are absorbed by inner-shell excitation of atoms involved in the deep-level defect center. If the trapped electron refills the shell of the excited atom, one would observe an optically stimulated carrier emission.

The time constant for changes of trap occupation by photon absorption is related to the optical cross section and τ by

$$\tau=(\sigma\phi)^{-1}, \tag{3}$$

where σ is the x-ray absorption cross section of the atom and ϕ is the local photon flux at the defect. The expected time constants for process (a) can be calculated based on the reported data. The absorption cross section of arsenic at the K edge is $\sigma=2\times10^{-20}$ cm^2.[32] The integral monochromatic flux on the sample was 10^9 photons mm^{-2} s^{-1}, which leads to a time constant of

$$\tau\approx5\times10^8 \text{ s}.$$

Such a time constant (of the order of 10 yr) is beyond the time scale of our experiments. Even if we underestimated the photon flux by a few orders of magnitude, the time constant is still inconsistent with the experimental results. The same is true for the experiments of Ishii;[15] the flux onto the sample is not specified in this paper, but the website of the Spring8 facility[33] gives the flux onto the sample achievable at the BL10XU beam line as $>10^{13}$ s^{-1}.

On the other hand, transient effects also occur if minority charge carriers are drifting throughout the depletion layer and are captured by defects filled with majority carriers. This absorption process is schematically shown in Fig. 7(b). The excited core hole creates many electron-hole pairs which diffuse through the sample. Minority carriers diffuse and drift to the deep-level defects in the space-charge region of the Schottky barrier diode. The time constant for trapping the minority carriers is given by Shockley-Read-Hall (SRH) statistics as

$$\tau=\frac{qv_{drift}}{c_p j_{photo}}, \tag{4}$$

where q is the elementary charge, v_{drift} the drift velocity inside the depletion layer, j_{photo} the photocurrent density, and c_p is the hole capture coefficient. The drift velocity depends on the linearly varying electrical-field strength in the depletion layer. For doping densities of 10^{17} cm^{-3}, the drift velocity for holes is close to the saturation value of about 2×10^7 cm s^{-1}. With the measured photocurrent density $j_{photo}\approx2\times10^{-7}$ A cm^{-2} , the capture coefficient for hole capture, $c_p=5.5\times10^{-8}$ cm^3 s^{-1},[19] and Eq. (4) we obtain, a value very similar to our experimentally observed time constants given, e.g., in Fig. 3,

$$\tau\approx300 \text{ s}.$$

We want to emphasize that the capacitance transients are not the cause for changes in the steady-state capacitance discussed in the proceding section. Under continuous irradiation, the transients result in a monotonic change in occupation as well as in capacitance, and therefore cannot explain any oscillatory changes observed in the steady-state capacitance. The steady-state capacitance oscillation is only due to the presence of the photocurrent from the absorption of x rays and can be observed even in completely defect-free space-charge junctions. Yet, capacitance transients only occur if deep-level centers are present. For reliable scanning measurements of the steady-state capacitance, care has to be taken at the start of the measurement, because some transient behavior of the deep-level occupation toward the steady state may induce erroneous results.

C. Site selectivity of capacitance XAFS

In the above section we have discussed and explained the photocurrent and capacitance changes induced by the x-ray irradiation and show that not all the processes will give a site selectivity of the XAFS as proposed by Ishii and co-workers.[13–15] In this section, we want to discuss only those processes which could lead to the suggested site selectivity.

1. Possible processes for a site-selective detection of XAFS

The basic principle of the proposed site selectivity is that only those inner-shell excitations are detected which belong to a specific defect site. Ishii and co-workers associate the x-ray absorption at an inner shell with an occupancy change of a defect level at the same atom. Besides the direct x-ray absorption from the defect level, which has no connection to the inner-shell absorption, only process (a) in Fig. 7 will lead to the proposed site selectivity. The x-ray photons excite the K-shell electron which leaves the atom, and the electron trapped in the defect level fills the core hole. The detection of the photocapacitance could in principle reveal the charge state change at the defect level. However, the discussion given in Sec IV B 3 showed that this process is not effective in changing the capacitance. The only way to account for the large capacitance changes is by including the effect of the photocurrent on the capacitance. The photocurrent, however, is associated with the electron-hole pairs created by impact ionization. During the ionization process and through diffusion the electron-hole pairs loose their site selectivity and the photocurrent detection of XAFS gives the same results as the transmission or fluorescence measurements. It is obvious from these arguments why the photocapacitance and the photocurrent change due to x-ray irradiation leads to the same XAFS results. In both cases, the changing occupancy of the defect level is associated with the photocurrent.

Photocapacitance transients of process (a) in Fig. 7 remain another possible way to achieve a site-selective detection of XAFS. A clear capacitance transient was measured during the inner-shell absorption process (Sec III A). The determined time constants, however, are indicative of a minority carrier recombination. The direct relaxation of the defect electron occurs with much larger time constants (see the discussion in Sec. IV B 4). Again, the minority carriers originate from the photocurrent, which is not site selective.

2. Host absorption versus direct absorption at the defect

In general, part of the x-ray irradiation is absorbed directly by the defects. In case of the AlGaAs samples, these are arsenic or gallium atoms which are related to the DX centers. As the microscopic environment of these atoms is different compared to undisturbed lattice positions, the fine structure is expected to differ, but the magnitude of the absorption coefficient remains the same. Under the assumption of a trap ionization by x-ray absorption at atoms on defect site and a corresponding capacitance change of the depletion layer, one can estimate the expected photocurrent of the site-selective absorption process.

The photocurrent (which is not site selective) is due to the absorption at about 10^{22} cm^{-3} host atoms. The concentration of DX centers in the samples was 10^{16} cm^{-3}, i.e., six orders of magnitude smaller than the concentration of bulk atoms. The photocurrent from the defect atoms is therefore smaller by six orders of magnitude and impossible to detect. The capacitance transient measurements have shown that the trap ionization can only be explained by a hole capture from the photocurrent and not by direct site-selective absorption processes. Thus, the capacitance XAFS gives the same information as the photocurrent measurements. As all electrical detection techniques are based on the photocurrent, it is always the absorption fine structure of the bulk material that is determined, not that of defects. All our results can be qualitatively as well as quantitatively explained by the hole capture from the photocurrent. Thus, the time constant vs x-ray energy obtained from XAFS contain the same information as the photocurrent spectra.

3. Other detection schemes

The capacitance technique has been further developed to include capacitance detection from a scanning probe using an atomic force microscope[34,35] and the detection of XAFS oscillation in the channel of field-effect transistor (FET) devices.[14] In both cases the measured x-ray-induced capacitance changes can be attributed to the same processes that are discussed above. Our explanation of the cause of the capacitance changes relies only on general principles of semiconductor physics, such as the excitation of a photocurrent and SRH statistics. It is completely independent of the way detection is achieved. This also applies to the case of capacitance XAFS measurements using an AFM or on FET structures. No site selectivity is expected.

The suggested improved spatial resolution is also in doubt. Indeed, it is the diffusion length of the photoexcited carriers that determines the resolution, and not the tip radius of the atomic force microscope or the dimensions of the FET channel.

X-ray excited optical luminescence detection (XEOL-XAFS) of the fine structure was also proposed to show site selectivity.[36,37] Transparent rare-earth compounds doped with other rare-earth atoms are excited by x rays. The optical luminescence from the rare-earth atoms originates from intra $4f$-shell transitions, which should be effectively shielded against the solid. The energy transfer from the solid to the ion is less efficient, so that the conditions for site selectivity is more favorable. But even in this case, detailed studies have shown that site selectivity cannot be achieved with XEOL-XAFS.[38] The fact that the optical signal arises from a different atom than the absorbing atom was demonstrated for Gd_2O_2S:Tb excited by x-ray photons at the Gd edge. In multicrystalline samples, different structural phases could be detected, due to the hindered energy transfer from one phase to the other.[39] But even in this simple case, the site selectivity of XEOL-XAFS was questioned.

V. SUMMARY

We have used different techniques for the detection of x-ray absorption oscillations near the absorption edges of Ga and As atoms in GaAs and AlGaAs. From our analysis of the experimental XAFS spectra we find no evidence for a site selectivity of electrical, in particular, capacitance detection of XAFS. Instead, we present strong arguments against such a selectivity. The advantage of the electrical technique is the large signal-to-noise ratio that can be best realized by measuring the photocurrent. Capacitance measurements are not site selective and give the same results but with an unfavorable low signal-to-noise ratio.

ACKNOWLEDGMENTS

We acknowledge the stimulating discussions with R. Sielemann, who initiated this study. A.W.R Leitch, University of Port Elizabeth, SA, supplied the AlGaAs samples and P. Gladkov prepared the contacts on the GaAs samples. Valuable and numerous discussions with D. Meyer on the XAFS technique are acknowledged. The work was funded by the BMBF under Contract No. 05KK10DA/2.

---

*Electronic address: joachim.bollmann@physik.tu-dresden.de

[1] E.A. Stern, Phys. Rev. B **10**, 3027 (1974).

[2] F.W. Lytle, D.E. Sayers, and E.A. Stern, Phys. Rev. B **11**, 4825 (1975).

[3] V.L. Aksenov, A.Y. Kuzmin, J. Purans, and S.I. Tyutyunnikov, Phys. Part. Nucl. **32**, 675 (2001).

[4] *X-ray Absorption: Principles, Applications, Techniques of EXAFS, SEXAFS, and XANES*, edited by D. C. Koningsberger and R. Prins (Wiley, New York, 1988).

[5] J. Mustre de Leon, J.J. Rehr, S.I. Zabinsky, and R.C. Albers, Phys. Rev. B **44**, 4146 (1991).

[6] J.J. Rehr, R.C. Albers, and S.I. Zabinsky, Phys. Rev. Lett. **69**, 3397 (1992).

[7] S. Wei, H. Oyanagi, H. Kawanami, K. Sakamoto, T. Sakamoto, and N.L. Saini, J. Synchrotron Radiat. **6**, 573 (1999).

[8] V. Koteski, N. Ivanovic, H. Haas, E. Holub-Krappe, and H.-E. Mahnke, Nucl. Instrum. Methods Phys. Res. B **200**, 60 (2003).

[9] D. K. Schroder, *Semiconductor Material and Device Characterization* (Wiley, New York, 1990).

[10] D.V. Lang, J. Appl. Phys. **45**, 3023 (1974).

[11] M. Knupfer, R. Neuder, M. Kielwein, S. Haffner, M.S. Golden, J. Fink, C. Kim, Z.-X. Shen, M. Merz, N. Nücker, S. Schuppler, N. Motoyama, H. Eisaki, S. Uchida, Z. Hu, M. Domke, and G. Kaindl, Phys. Rev. B **55**, R7291 (1997).

[12] M. Merz, N. Nücker, P. Schweiss, C.T. Chen, V. Chakarian, J. Freeland, Y.U. Idzerda, M. Kläser, G. Müller-Vogt, and T. Wolf,

Phys. Rev. Lett. **80**, 5192 (1998).
[13] M. Ishii, Y. Yoshino, K. Takarabe, and O. Shimomura, Appl. Phys. Lett. **74**, 2672 (1999).
[14] M. Ishii, J. Appl. Phys. **40**, 7219 (2001).
[15] M. Ishii, Phys. Rev. B **65**, 085310 (2002).
[16] D.V. Lang, R.A. Logan, and M. Jaros, Phys. Rev. B **19**, 1015 (1979).
[17] P.M. Mooney, Semicond. Sci. Technol. **6**, B1 (1991).
[18] M. Kaminska, Rev. Phys. Appl. **23**, 793 (1988).
[19] M.A. Zaidi, H. Maaref, and J.C. Bourgoin, Appl. Phys. Lett. **61**, 2452 (1992).
[20] S. Duenas, E. Castan, A. Dios, L. Bailon, J. Barbolla, and A. Perez, J. Appl. Phys. **67**, 6309 (1990).
[21] For details, see www-hasylab.desy.de
[22] R. Brunwin, B. Hamilton, P. Jordan, and A.R. Peaker, Electron. Lett. **15**, 349 (1979).
[23] M. Newville, P. Livins, Y. Yacoby, J.J. Rehr, and E.A. Stern, Phys. Rev. B **47**, 14 126 (1993).
[24] J.J. Rehr, J. Mustre de Leon, S.I. Zabinsky, and R.C. Albers, J. Am. Chem. Soc. **113**, 5135 (1991).
[25] New Series, Group 3, Vol.41, Pt. A1α *Numerical Data and Functional Relationships in Science and Technology*, Landolt-Börnstein, (Springer, Berlin, 2001).
[26] V. Koteski, B. Reinhold, H. Haas, E. Holub-Krappe, H.-E. Mahnke, and D. Wruck, Hyperfine Interact. **136/137**, 681 (2001).
[27] H. Fricke, Phys. Rev. **16**, 202 (1920).
[28] G. Hertz, Z. Phys. **3**, 19 (1920).
[29] R.F. Boehme, G.S. Cargill, III, W. Weber, and T. Jackson, J. Appl. Phys. **58**, 811 (1985).
[30] T.D. Hu, Y.N. Xie, S. Qiao, Y. Hai, Y.L. Jin, and D.C. Xian, Phys. Rev. B **50**, 2216 (1994).
[31] W.J. Stepowicz, Solid-State Electron. **20**, 817 (1977).
[32] See www.physics.nist.gov/PhysRefData/FFast/html/form.html
[33] For details, see www.spring8.or.jp
[34] M. Ishii, Physica B **308–310**, 1153 (2001).
[35] M. Ishii, Nucl. Instrum. Methods Phys. Res. B **199**, 205 (2003).
[36] A. Bianconi, D. Jackson, and K. Monahan, Phys. Rev. B **17**, 2021 (1978).
[37] J. Goulon, P. Tola, M. Lemonnier, and J. Dexpert-Ghys, Chem. Phys. **78**, 347 (1983).
[38] L. Soderholm, G.K. Liu, M.R. Antonio, and F.W. Lytle, J. Chem. Phys. **109**, 6745 (1998).
[39] R.F. Pettifer and A.J. Bourdillon, J. Phys. C **20**, 329 (1987).